



**HAL**  
open science

# Sector Entry Flow Prediction Based on Graph Convolutional Networks

Chunyao Ma, Sameer Alam, Qing Cai, Daniel Delahaye

► **To cite this version:**

Chunyao Ma, Sameer Alam, Qing Cai, Daniel Delahaye. Sector Entry Flow Prediction Based on Graph Convolutional Networks. International Conference on Research in Air Transportation, Jun 2022, Tampa, United States. hal-03701661

**HAL Id: hal-03701661**

**<https://enac.hal.science/hal-03701661>**

Submitted on 22 Jun 2022

**HAL** is a multi-disciplinary open access archive for the deposit and dissemination of scientific research documents, whether they are published or not. The documents may come from teaching and research institutions in France or abroad, or from public or private research centers.

L'archive ouverte pluridisciplinaire **HAL**, est destinée au dépôt et à la diffusion de documents scientifiques de niveau recherche, publiés ou non, émanant des établissements d'enseignement et de recherche français ou étrangers, des laboratoires publics ou privés.

# Sector Entry Flow Prediction Based on Graph Convolutional Networks

Chunyao Ma\*, Sameer Alam\*, Qing Cai\*, Daniel Delahaye†

\*Air Traffic Management Research Institute, School of Mechanical and Aerospace Engineering

Nanyang Technological University, Singapore

†OPTIM Lab, Ecole Nationale de l'Aviation Civile, Toulouse, France

Email: \*M180146@e.ntu.edu.sg, {\*sameeralam| \*qcai}@ntu.edu.sg,

†daniel.delahaye@enac.fr

**Abstract**—Improving short-term air traffic flow prediction can help forecast demand and maximize existing capacity by tactical air traffic flow management. Most existing studies in flow prediction lacks consideration of the dynamic, structural, and interrelated nature of air traffic flows in the airspace. Therefore, this paper proposes to predict sector entry flows based on graph convolutional networks, which consider the dynamic spatial-temporal features of air traffic from a graph perspective. First, we specify a sector entry flow based on its upstream and downstream sectors. Then, each entry flow is denoted as a node in a graph. The weighted edges between the nodes are learned from a Word2vec model based on air traffic flows among the nodes. With the weighted graph constructed and the temporal flows on the nodes extracted from the flight trajectories, an Attention-based Spatial-Temporal Graph Convolutional Network (ASTGCN) module is adopted to capture spatial-temporal features of recent, daily-periodic, and weekly-periodic flows in the graph. Finally, The outputs from the ASTGCN module based on the three features are fused to generate the final prediction results. The proposed method is applied on 164 sectors of French airspace for one-month ADS-B data (from Dec 1, 2019, to Dec 31, 2019) which includes 158,856 flights. Results show that, the proposed method outperforms the well established Long short-term memory (LSTM) model, and demonstrates better capability in predicting rapid changes in traffic flow and has relatively smaller decrease in prediction accuracy as the prediction time-window increases.

**Index Terms**—air traffic, flow prediction, graph convolutional network, spatial-temporal.

## I. INTRODUCTION

Controlled airspace around the world is reaching its operational capacity as air transportation grows both physically and operationally [1]. One of the key challenge confronted by air navigation service providers (ANSPs) is the imbalance between the limited airspace capacity and the increasing traffic demand, which is the major source of air traffic congestion that leads to traffic delays, economic losses, and potential safety issues [2]. Although passenger demand during the outbreak of the COVID-19 pandemic almost came to a standstill, with traveling restrictions are being lifted gradually, air traffic demand is now on its way to ramping up [3]. This brief pause for the air transportation industry could also be an opportunity to develop and adopt new approaches to accommodate future air traffic growth.

In the presence of limited capacity, an accurate short-term air traffic flow prediction, i.e., 0-2 hour look ahead time [4], in the airspace can be vital for Air Traffic Controllers (ATCs) about managing the forthcoming traffic flow situation and evaluating of control strategies [5]. In this way, tactical Air Traffic Flow Management (ATFM) [6] measures can be planned and executed in advance in a more efficient manner to maximize the use of the existing airspace capacity [7]. For instance, ATCs can execute the agreed tactical measures, such as traffic re-routing and flight level allocation, in advance, to provide a smooth and efficient flow of traffic where demand is foreseen to exceed capacity or disruptions such as convective weather appears, to utilize the available capacity to the maximum extent [8].

## II. RELATED LITERATURE

In current literature, there are mainly two types of short-term air traffic flow modelling and prediction methods, i.e., trajectory-based method and aggregate method. Trajectory-based air traffic flow prediction is based on propagating the flight trajectories over time and using the predicted trajectories to count the future number of flights in the airspace [9]. However, research shows that the prediction error of the trajectory-based method increases exponentially as the forecast time horizon increases beyond 20 minutes, which may be caused by its sensitivity to various influencing factors, such as weather conditions, airspace restrictions, and human factors [10]. Furthermore, the dimension of the trajectory-based method depends on the number of flights under consideration, which can requires huge computational costs and make such methods untenable in real world context.

Efficient ATFM demands prediction of the overall traffic flow situations in the specified airspace, instead of the temporal trajectory of individual aircraft. Thus, the aggregate air traffic flow models focus on predicting the overall distributions of the air traffic flow in the airspace [11]. Since flights in the airspace are spatially aggregated, the computational cost can be reduced significantly comparing to the trajectory prediction based approaches. Moreover, without considering the individual behaviours of flights, the aggregated prediction methods are less sensitive to the uncertainty factors related to individual

flights and a longer forecast time horizon with less prediction errors can be achieved.

Recently, the aggregated approach is widely discussed in the literature, which mainly predict air traffic flow based on probabilistic analysis or machine learning techniques. Based on the flights transition probability between adjacent air traffic control centers, a stochastic framework with Linear Dynamic System Model (LDSM) was developed by Sridhar et al [8]. The traffic flow is predicted as the flights count in each control center during a short term, e.g., a few hours, using the flights transition probability between adjacent centers extracted from historical data, the number of departure/arrival flights in the control center and the departure uncertainties. The major shortcoming of the stochastic framework is that it adopts Poisson distributions to model the departures at each time step, ignoring the fact that the departure traffic flow varies significantly during days, weeks and seasons under different traffic conditions. Gilbo et al. further explored the stochastic LDSM to predict the air traffic flow at the sector levels using a linear regression model [12]. However, their research mainly focused on improving the flow prediction results of the Enhanced Traffic Management System, without deeper investigation of the prediction mechanism of air traffic flow prediction.

Probabilistic based models for flight or airspace were also studied to illustrate stochastic features, such as flight speed and traffic density, of the air traffic and further used to predict the traffic flow [13]. However, the performances of probabilistic methods are affected by handcraft models or analyses, which makes it difficult to fully depict the real traffic situation and capture the sharp changes in the highly dynamic traffic flow.

In recent years, machine learning algorithms are started to be implemented in aggregated air traffic flow prediction [14]. In [4], the authors discretized the airspace into small cubes and predicted the flight count in each cube. The prediction was achieved by a convolutional neural network and recurrent neural network to model the spatial and temporal correlations of air traffic flow. The main shortcoming of this model is that the disintegration of airspace into cubes ignores the structural features of the airspace, such as airway network structure and sectorisation schemes. This may limit the practical implementation of the prediction results in ATFM. In [15], the authors adopted a Phase-Space Reconstruction Extreme Learning Machine (PSR-ELM) model to learn and predict the time series of traffic demand passing given waypoints in the airspace. In [16], by exploring ADS-B data, the authors adopted long Short-Term Memory (LSTM) and Support Vector Machine (SVM) to predict the air traffic demand between two airports. The limitation of such time-series models is that they fail to consider the effects that the air traffic network has on time-series flow at a single waypoint or airport pair, which may restrain the prediction accuracy of the models [17].

Note that most of the current literature in air traffic flow prediction lacks considerations of the highly dynamic, structural and interrelated nature of air traffic flows in the airspace, such as considering the air traffic flow at different positions in

the airspace as different time-series isolated from each other. This paper proposes to predict sector entry flows based on a graph-represented structure of air traffic, which intrinsically considers the dynamic spatial-temporal evolution of air traffic from a graph perspective. First, the sector entry flow prediction is formulated as a three-stage-flow prediction problem, which considers three stages of an entry flow: the upstream sector, the entry sector, and the downstream sector. Each sector entry flow is then represented by a node in the graph. Further, the interactions among the entry flow in the airspace are described by the weighted edges between nodes, which is modelled by a Word2vec neural network [18] using the sequences of traffic flow transitions among the nodes. With the weighted graph constructed and the temporal flows on the nodes extracted from the flight trajectories, an Attention-based Spatial-Temporal Graph Convolutional Network (ASTGCN) module is adopted to capture spatial-temporal features of recent, daily-periodic, and weekly-periodic air traffic flows in the airspace. The outputs from the ASTGCN module based on the recent, daily, and weekly historical data are fused to predict the traffic flow on the nodes (sector-entry).

### III. PROBLEM DESCRIPTION

A sector's capability in handling air traffic is not only determined by the number of the flights that can be served, but also influenced by the traffic complexity inside the sector, such as flight distributions and flight speeds [19], [20]. Thus, besides predicting the number of future flights entering a sector, it is also essential for air traffic flow predictions to provide the distribution of the upcoming traffic flow of the sector, such as the number of flights crossing the entry/exit points of the sector, the number of flights transiting through the air routes in the sector, or the number of flight passing certain waypoints in the sector.

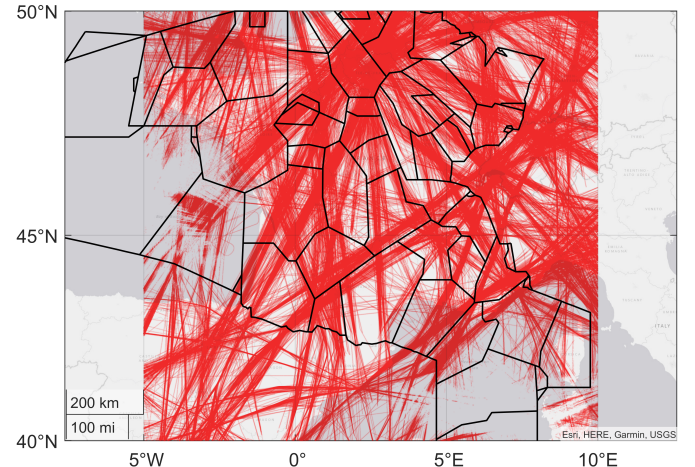


Fig. 1: Visualization of one-day flight trajectories in French airspace.

In recent years, the gradual implementation of Free Route Airspace (FRA) gives flights some freedom to plan their routes between an entry point and an exit point without referring

to the ATS routes [21]. Fig. 1 shows the one-day flight trajectories (red lines) in French airspace (sector boundaries shown as black lines), where the FRA has been implemented in nearly 50% of the airspace above flight level 195 [22]. It can be observed from Fig. 1 that the majority of flight trajectories follows straight path and do not follow specific air routes in the airspace. The entry/exit points of flights into a sector are no longer fixed at certain positions at the sector boundary. Under this context, it is however impractical to predict air traffic flow on airways, fixed entry/exit points on sector boundaries, or waypoints.

Note that in the FRA, flights will remain subject to control from the sector ATCs. We can notice from Fig. 1 that most of the flows entering a sector are aggregated by their upstream and downstream sectors. Therefore, predicting the number of flights in the entry flow along with downstream and upstream information, i.e., where the flow is from and where it is going to, can provide ATCs an understanding of the emerging flow in a sector to develop flow control strategies.

Given the above analysis, this paper aims to predict the number of flights in the sector entry flows. An entry flow of a sector is defined as the flow entering the sector in which the flights have the same upstream and downstream sector. The prediction outcome will be the number of flights in each sector entry flow during a look-ahead time. For instance, flow “S1S2S3” represents one entry flow to Sector “S1”, which is from Sector “S2” and going to Sector “S3”. And this paper proposes to predict the number of flights in flow “S1S2S3” during a given look-ahead time.

## IV. METHODOLOGY

### A. Methodology Overview

The proposed method to predict the sector entry flows comprises seven steps. The first step denoises the raw ADS-B data. The second to fourth steps organize the denoised ADS-B data and airspace structure data into a spatial-temporal graph. The rest three steps build the machine learning framework to learn from the spatial-temporal traffic information and make predictions about future traffic flow.

The flight information used in the paper is extracted from ADS-B data. It faces plenty of noises in measuring barometric altitudes, which is susceptible to variations in atmospheric conditions [23]. Therefore the first step is to remove the noises from the barometric altitude data. From the denoised ADS-B data, 4D trajectories of the flights is obtained i.e., time series data with geographic information. Therefore, in the second step, by referring to the airspace structure data, i.e., sector boundaries, we can map each 4D trajectory into a sequence of nodes at sectors boundaries and determine the corresponding times when the flight passes the nodes. In the third step, the nodes sequences are fed to a Word2vec model, which extracts the notion of relatedness across nodes and encodes each node into a numerical vector. By calculating the similarity between the vectors, we can quantify the relatedness between nodes, i.e., weights on the edges connecting the node pairs. In the fourth step, a spatial-temporal graph is built to describe the

flow of air traffic in the airspace by combining the times series of flights on each node with the weights on the edges between nodes.

Based on the spatial-temporal graph established in the previous four steps, the last three steps adopt a graph-based neural network to achieve the prediction of the sector entry flow. Step five organizes the spatial-temporal graph obtained in step 4 into a time series sliding over different time slices, from which the weekly, daily, and recent flow features can be extracted. Step six adopts an ASTGCN module to capture the dynamic spatial and temporal patterns from the weekly, daily, and recent data. And in the seventh step, the outputs from the ASTGCN module of the three features are fused to obtain the air traffic flow prediction for the future time slices.

Following subsections details about data denoising, spatial-temporal graph construction, and the graph-based neural network to learn and predict air traffic flow.

### B. Data Denoising

ADS-B data for aircraft surveillance can give highly accurate aircraft position and velocity information, providing a useful source for analytical solutions to effective and efficient airspace usage [24]. However, ADS-B data still includes some noise in flights’ geographic information, especially barometric altitude [25]. The black line in Fig. 3 shows a flight trajectory extracted from the ADS-B data. Many spikes are observed in different phases of the flight, especially in take-off, cruise, and landing. This section will describe removing these spikes from the flight trajectory.

To remove the spikes from the cruise phase data, we adopt a median filter [26] that moves through the trajectory data one by one; and replaces each value with the median value of its neighboring data. The green line in Fig. 3 shows the denoised flight trajectory, in which the spikes in the cruise phase are smoothed after applying the median filter.

However, We cannot wholly flatten the noise in the altitude data by using a median filter, as a spike can still be observed at the initial part of the green curve. The cause of the altitude data busts during the take-off/landing phase may be the failure to change the necessary QNH [27] setting during the take-off/landing phase to the correct altimeter setting [28]. Thus, during the take-off/landing phase, the outlier data constantly show up over a relatively long time window, compared to the cruise phase during which the outlier data appear individually and are easy to be removed through a median filter. Given the constant occurrence of inaccurate barometric altitude data during take-off/landing, it is better to remove the trajectory data during these phases, i.e., below a certain flight level threshold, to avoid influencing the reliability of the research results. Therefore, we apply Robust Locally Weighted Scatterplot Smoothing (RLOWESS) [29], which uses locally weighted linear regression to smooth data, onto the filtered data (green line) to fit a smooth curve from which we can identify the overall trend of the trajectory. The blue line in Fig. 3 shows the smoothed curve after applying RLOWESS. By removing the corresponding data in the green line below a certain flight

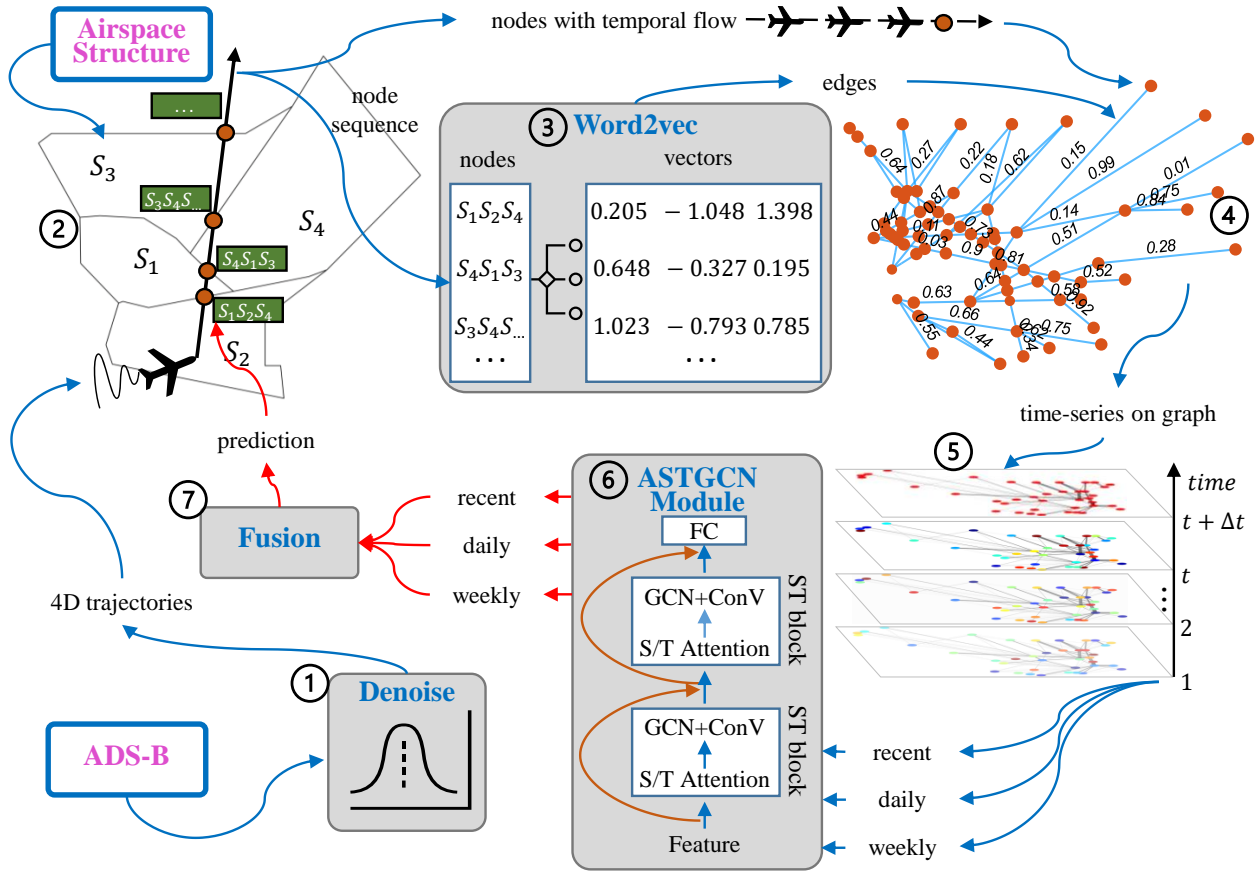


Fig. 2: Conceptual diagram of the proposed method for short-term sector entry flow prediction based on graph convolutional networks.

level (above which the flight altitude measurement is stable) indicated by the blue line, we can get the final denoised flight trajectory, shown by the red curve in Fig. 3.

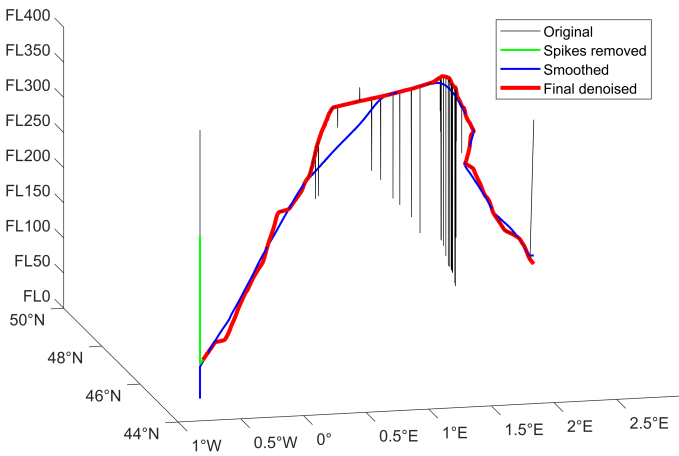


Fig. 3: Illustration of the proposed ADS-B data denoising approach.

### C. Spatial-temporal Graph Construction

This section organizes the denoised flight trajectories and the airspace structure information into a spatial-temporal graph representation  $G = (V, E)$ , where  $V$  is the set of nodes in the graph, and  $E$  is the set of edges indicating the connectivity between the nodes. This section consists of nodes extraction, edges generation, and graph construction.

1) *Nodes Extraction:* From the ADS-B data, 4D flight trajectories, containing the geographic information of flights over time, can be obtained. By intersecting the 4D flight trajectories with sector boundaries, it can be determined where and when a flight enters into each sector. An entry point of a flight into a sector can be described as a node defined by the entry sector, the upstream sector, and the downstream sector. More specifically, when a flight  $f_k$  enters sector  $S_i$  from sector  $S_{i-1}$  then goes to sector  $S_{i+1}$ , it belongs to the entry flow of sector  $S_i$  described by the node  $S_iS_{i-1}S_{i+1}$ .

Fig. 4 presents an example of nodes extraction from the trajectory of three flights. Flight  $f_1$  and  $f_2$  enter sector  $S_1$  from sector  $S_2$ , then go to sector  $S_3$ . Therefore, according to the definition of entry flow in the Problem Description section, the two flights belong to the entry flow of sector  $S_1$  represented by the node  $S_1S_2S_3$ . Similarly, upon entering sector  $S_3$ , the two flights are classified to the entry flow of  $S_3$  represented by

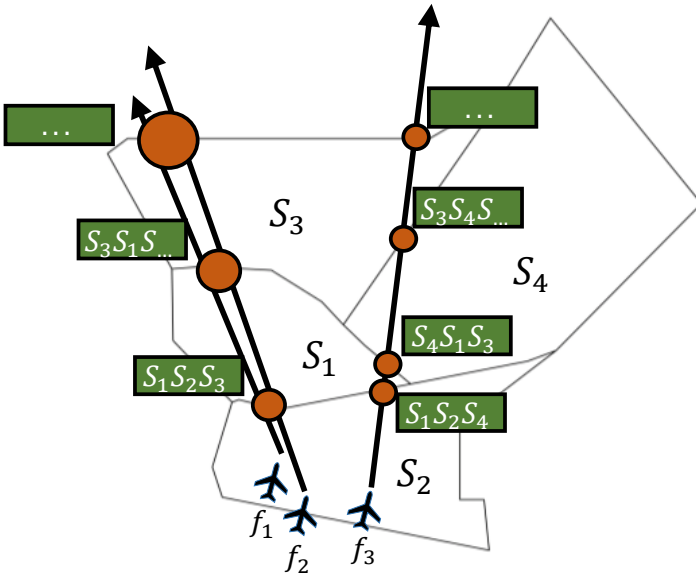


Fig. 4: An example of nodes extraction from the trajectory of three flights.

the node  $S_3S_1S_{...}$ , while  $S_{...}$  represents the subsequent sector after exiting  $S_3$ . In the same way, the nodes passed by flight  $f_3$  are  $S_1S_2S_4$ ,  $S_4S_1S_3$ , and  $S_3S_4S_{...}$ , when entering sector  $S_1$ ,  $S_4$ , and  $S_3$ , respectively. By identifying the nodes from each flight trajectory in the ADS-B data, we can determine all the nodes in the traffic graph.

2) *Edges Generation*: After determining the nodes, the next step is to construct the edges between the nodes. In this study, if two nodes are passed by a flight consecutively, they will be considered connected, and there will be an edge between them. Most current research in graph convolutional networks for traffic flow prediction either adopts a binary graph [30] or set the edge weights according to the geometric distance between the nodes [31]. However, these simple representations of the weights may fail to capture many complex features in the graph, e.g., some edges are frequently traveled while some are seldom used, which may limit the ability of graph convolutional networks to learn from the features of neighboring nodes [32]. Therefore, instead of adopting a simple representation of the weights, this paper proposes to learn the edge weights through the traffic data, i.e., the sequences of nodes generated from each flight trajectory.

Word2vec is a technique for natural language processing published in 2013 [18]. It uses a neural network to model word associations by training from a text corpus. In this process, Word2Vec can build a vocabulary from the training text corpus and learn the vector representations of each word. The cosine similarity between the vectors can indicate semantic similarity between the words represented by those vectors [33].

Making an analogy between a node sequence and a text sentence with the nodes being the words in the sentence, the set of node sequences generated from the flight data can be regarded as the text corpus. Thus, by feeding the node

sequences to a Word2vec model, we can obtain the vector representation for each node. Subsequently, the edge weights between nodes can be described by the cosine similarity between the corresponding vectors. In this way, the weighted edges between the nodes in the graph are determined.

3) *Graph Construction*: We have determined the nodes and edges for a graph in the previous two steps. For each node, based on the time of each flight passing it, we associate it with a time-varying traffic flow described by a sequence of flights on the temporal dimension. More specifically, if flights  $f_1, f_2, \dots, f_k$  pass the node  $S_iS_{i-1}S_{i+1}$  at an increasing sequence of time  $t_1, t_2, \dots, t_k$ , the temporal flow on node  $S_iS_{i-1}S_{i+1}$  can be represented by a sequence  $\{(f_1, t_1), (f_2, t_2), \dots, (f_k, t_k)\}$ . The nodes with dynamically changing flow and the weighted edges between nodes constitute the spatial-temporal graph structure.

#### D. Sector Entry Flow Prediction

Given the spatial-temporal graph constructed in the last step, this section predicts the flows, i.e., the number of flights, passing the nodes in the graph during a future time slice.

With the temporal flight sequence recorded on each node in the graph  $G$ , we can determine a traffic flow time series for each node over different time slices. We use  $x_t^i \in R$  to denote the traffic flow of node  $i$  at time  $t$ .  $\mathbf{X}_t = (x_t^1, x_t^2, \dots, x_t^N)^T \in R^N$  denotes the traffic flow values of all nodes at time  $t$ .  $N$  is the number of nodes in the graph.  $\chi = (\mathbf{X}_1, \mathbf{X}_2, \dots, \mathbf{X}_\tau)^T \in R^{N \times \tau}$  denotes the traffic flow values of all nodes over  $\tau$  time slices. Therefore, the air traffic flow prediction problem can be specified as: given  $\chi$ , traffic flow values at all the nodes on the graph over past  $\tau$  time slices, predict future traffic flow sequences  $\mathbf{Y} = (\mathbf{y}^1, \mathbf{y}^2, \dots, \mathbf{y}^N)^T \in R^{N \times T_p}$  of all the nodes on the whole traffic graph over the next  $T_p$  time slices, where  $\mathbf{y}^i = (x_{\tau+1}^i, x_{\tau+2}^i, \dots, x_{\tau+T_p}^i) \in R^{T_p}$  denotes the future traffic flow of node  $i$  from  $\tau + 1$  to  $\tau + T_p$ .

As shown in Fig. 2, this paper incorporate three time series features, i.e., recent flow series, daily flow series, and weekly flow series, to predict the future traffic flow. The three features are designed to respectively model the recent, daily-periodic and weekly-periodic dependencies of the historical data. Assume the sampling frequency is  $q$  times per hour, the current time is  $t_0$ , and the prediction window size is  $T_p$ . We extract three time series segments during the last  $T_h$  hours,  $T_d$  days and  $T_w$  weeks as the input of the recent, daily-period and weekly-period feature respectively. Details about the three time series segments are illustrated below.

The recent segment is a segment of historical data adjacent to the predicting period, which is designed to capture the influence of the recent traffic evolution on the future traffic flows. This recent flow segment can be specified as:  $\chi_h = (\mathbf{X}_{t_0-T_h \times q+1}, \mathbf{X}_{t_0-T_h \times q+2}, \dots, \mathbf{X}_{t_0}) \in R^{N \times S_h}$ , while  $S_h = q \times T_h$ .

The daily-periodic segment is a time series of traffic flow over the past few days during the same time period as the predicting period, which is designed to capture the daily repeated patterns of air traffic

flow. The daily segment can be specified as:  $\chi_d = (\mathbf{X}_{t_0-T_d \times 24q+1}, \dots, \mathbf{X}_{t_0-T_d \times 24q+T_p}, \mathbf{X}_{t_0-(T_d-1) \times 24q+1}, \dots, \mathbf{X}_{t_0-(T_d-1) \times 24q+T_p}, \dots, \mathbf{X}_{t_0-24q+1}, \dots, \mathbf{X}_{t_0-24q+T_p}) \in R^{N \times S_d}$ , while  $S_d = T_p \times T_d$ .

The weekly-periodic segment is composed of the flow series on last few weeks, which have the same week attributes and time intervals as the forecasting period. It is designed to capture the weekly repeated patterns of air traffic flow. The weekly segment can be specified as:  $\chi_w = (\mathbf{X}_{t_0-7T_w \times 24q+1}, \dots, \mathbf{X}_{t_0-7T_w \times 24q+T_p}, \mathbf{X}_{t_0-7(T_w-1) \times 24q+1}, \dots, \mathbf{X}_{t_0-7(T_w-1) \times 24q+T_p}, \dots, \mathbf{X}_{t_0-7 \times 24q+1}, \dots, \mathbf{X}_{t_0-7 \times 24q+T_p}) \in R^{N \times S_w}$ , while  $S_w = T_p \times T_w$ .

Each of the three time series feature will be fed to the ASTGCN module, shown in Fig. 2, respectively to model three temporal properties of air traffic flows. The ASTGCN module consists of a number of spatial-temporal blocks as well as a fully connected layer in the end to keep the output dimension the same as the forecasting target. A spatial-temporal block mainly consists of two mechanisms. First is the spatial-temporal attention mechanism which is employed to capture the dynamic spatial-temporal correlations in the traffic data. The second mechanism is the spatial-temporal convolution which uses graph convolutions and common standard convolutions to respectively capture the spatial dependencies from the neighborhood and the temporal dependencies from the time series. The spatial-temporal attention combined with the spatial-temporal convolution forms a spatial-temporal block. Multiple spatial-temporal blocks can be further stacked to capture larger range of dynamic spatial-temporal correlations.

Eventually, the outputs from the ASTGCN module based on each of the three features are weighted fused to generate the final prediction results of traffic flow on the nodes, depending on the significance of the influence of the three features. The final prediction result after the fusion can be described as:

$$\hat{Y} = W_h \circ \hat{Y}_h + W_d \circ \hat{Y}_d + W_w \circ \hat{Y}_w \quad (1)$$

where  $\circ$  represents the Hadamard product.  $W_h$ ,  $W_d$  and  $W_w$  are the learned parameters to quantify the influence of the three features on the forecasting target.

## V. EXPERIMENTAL STUDY

With the proposed method, we have carried out an experimental study on the French airspace using one-month ADS-B data from December 1, 2019 to December 31, 2019. A number of 158856 flights and 164 sectors in French airspace are included in the study. The prediction target is the hourly sector entry flows. The look ahead time investigated in this experiment ranges from 1 hour to 2 hours. The following sections presents the result of the experimental study.

### A. Graph Construction

By intersecting the flight trajectories with the sector boundaries in the French airspace, we have extracted 6028 nodes for the traffic graph to represent different entry flows of the 164 airspace sectors. From the sequence of nodes on a flight trajectory, we have determined the edges in the graph.

The sequences of nodes are further fed to the Word2vec neural network to model the edge weights. Fig. 5 shows the constructed graph for the French airspace. Each red node in the graph denotes a sector entry flow, and the node's size is proportional to the size of the traffic flow passing through it. Each blue line represents an edge in the graph, while the line thickness is proportional to the edge weight.

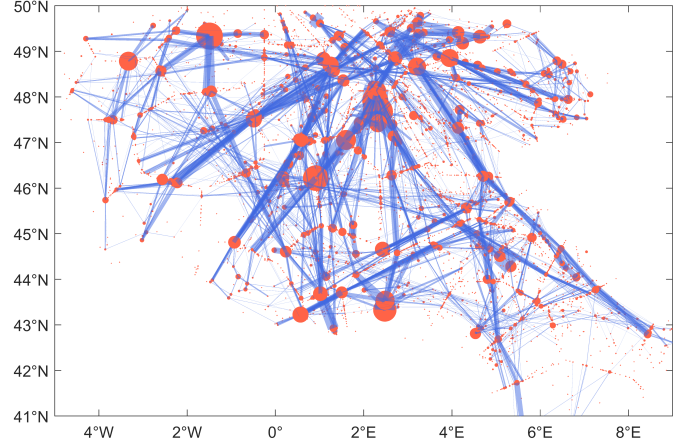


Fig. 5: The constructed graph for the French airspace. Each red node denotes a sector entry flow and each blue line denotes an edge in the graph.

### B. Sector Entry Flow Prediction

The last three hours, six days, one week flow features, i.e.,  $T_h = 3$ ,  $T_d = 6$  days and  $T_w = 1$ , of all nodes in the graph are extracted from the time series data and fed to the ASTGCN module to predict the next one hour to two hours traffic flows on the nodes. The ASTGCN module in this study adopts a widely used structure that stacks two spatial-temporal blocks. The mean square error (MSE) between the predicted and true values is used to compute the loss function of the model. The sampling frequency of the hourly flow on the nodes is set as 12 times per hour, i.e.,  $q = 12$ . The batch size is five during the training phase, and the learning rate is 0.0003. The training data, validation data, and test data consists of 60%, 20% and 20% of the whole data set respectively. Concretely, 18 days data are used for model training, the following 6 days data for model validation, and the last 6 days data for testing the model.

### C. Result Analysis and Comparison

We have compared the node flow prediction results of the proposed method with the state of art time series prediction model LSTM. Given there are over 6000 nodes in the graph, here we use a busy node in French airspace, node “LFBBP2-LFBBP1-LFBBP3”, as an example to present the prediction result on the test dataset. According the node definition, node “LFBBP2-LFBBP1-LFBBP3” represents an entry flow of sector “LFBBP2”, which is from sector “LFBBP1” and heading to sector “LFBBP3”.

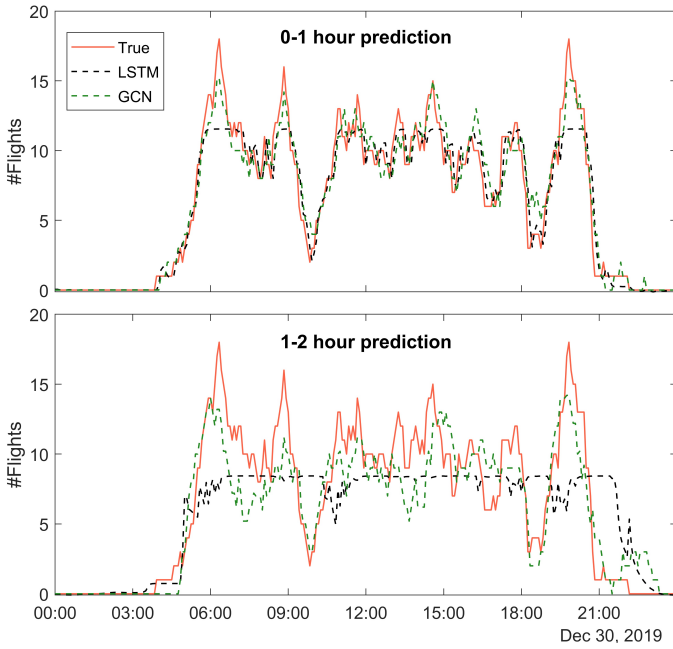


Fig. 6: Flow prediction result on node “LFBBP2-LFBBP1-LFBBP3” from 00:00 to 23:59 on Dec 30, 2019 (UTC). The upper panel plots the 0-1 hour prediction results, while the lower panel plots the 1-2 hours prediction results. The red solid shows the true flow values, the green dash shows the predicted values using the proposed GCN-based method, and the black dash shows the predicted value using LSTM.

TABLE I: Performance comparison between the proposed GCN-based method and the LSTM model using three metrics: MAE, MSE and RMSE.

Look ahead	Metric	GCN	LSTM
0-1 hr	MAE	0.864	0.887
	MSE	1.587	1.984
	RMSE	1.260	1.409
0.5-1.5 hr	MAE	1.402	2.016
	MSE	3.384	7.956
	RMSE	1.839	2.821
1-2 hr	MAE	1.784	2.535
	MSE	5.792	12.477
	RMSE	2.406	3.532

Fig. 6 presents the traffic flow prediction result from 00:00 to 23:59 on Dec 30, 2019. The upper panel plots the prediction results for the next 1 hour (0-1 hour), while the lower panel plots the prediction for the next 1-2 hours. The red solid shows the true number of flights passing node “LFBBP2-LFBBP1-LFBBP3”, the green dash shows the predicted value using the proposed method based on Graph Convolutional Networks (GCN), and the black dash shows the predicted value using LSTM. We can observe from Fig. 6 that both the proposed method and the LSTM model give forecasts that are close to the actual flow value in the coming 1 hour, while the proposed method can better capture the sharp increases in traffic flow. When the prediction window increases to 2 hours, the performance of the two models decreases. The

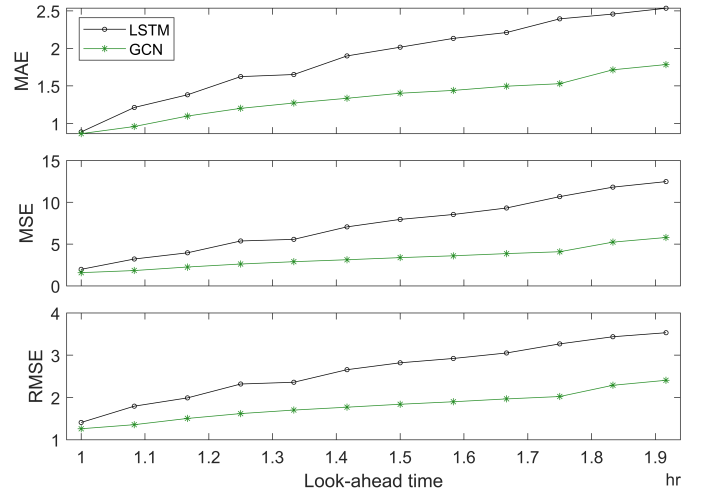


Fig. 7: Prediction performance (MAE, MSE and RMSE) changes of the proposed GCN-based method and the LSTM model as the prediction window increases.

performance of the LSTM model reduces sharply while the proposed method can still capture the trends of the traffic flow.

Table I shows the average performance comparison between the proposed method and the LSTM model, including three metrics: Mean Absolute Error (MAE), Mean Squared Error (MSE) and Root Mean Squared Error (RMSE). It can be seen from Table I that the proposed method achieves better performance in terms of all evaluation metrics. Fig. 7 shows the changes of prediction performance of the two models as the prediction window increases. Generally, when the prediction window is longer, the challenge of prediction becomes greater, consequently the prediction errors will increase. As can be seen from Fig. 7, LSTM can achieve good results in the short-term prediction. However, with the increase in the prediction window size, the prediction accuracy drops dramatically.

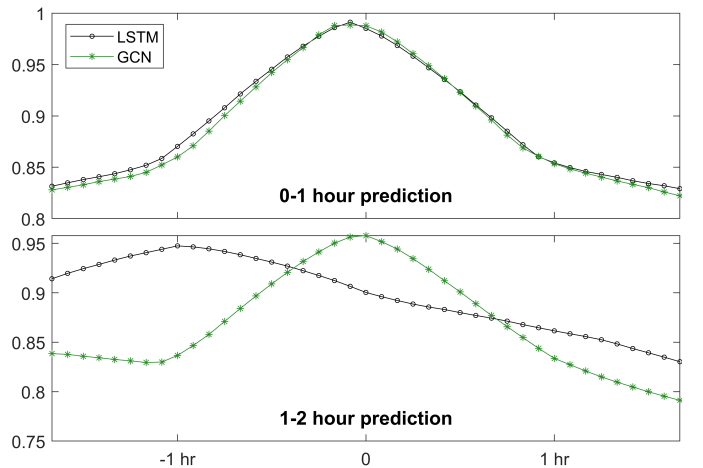


Fig. 8: Cross-correlation between the true values and the lagged (shifted) copies of predicted values. The horizontal axis shows the value of the time lag. The vertical axis shows the normalized value of the cross-correlation.

The reason of the sharp decrease in the performance of LSTM model may be that the LSTM model learns the correlations in the flow times series on the target node instead of the causal relationship between flows. Therefore its predictive power reduces sharply when trying to estimate the target at a later stage. As shown in Fig. 8, the predicted values using LSTM are highly correlated to the latest true value available in the input data. When the prediction window is 1 to 2 hours, we can observe a one-hour lag between the truth and the prediction of LSTM, while a zero-lag of the proposed method. The proposed method considers the spatial-temporal correlations which are more important in the long-term prediction. It has the potential to learn the causal relationship between flows from a graph perspective and produce good prediction results even when the prediction window is larger.

## VI. CONCLUSION AND DISCUSSION

This paper proposed a method for short-term sector entry flow prediction based on graph convolutional networks. Each entry flow of a sector was defined as a three-stage flow based on the entry, upstream, and downstream sectors. The prediction of each sector entry flow in the airspace was modelled as the prediction of temporal features on each node in a graph. We adopted a Word2vec neural network to model the interactions among the sector entry flows in the airspace, i.e., the weighted edges between nodes, based on the transition of air traffic in the graph. The weighted graph and the temporal flow series (hourly, daily, and weekly flows) on the nodes were input to an ASTGCN module to capture spatial-temporal dependencies from historical data and produce the final flow prediction results. We carried out an experimental study using the proposed method in the 164 sectors of French airspace using the flight data from Dec 1, 2019, to Dec 31, 2019, including 158856 flights. Results showed that, compared with the LSTM model, the proposed method could better capture sharp increases in traffic flow. And as the prediction window increased, the proposed method had shown a slower drop in prediction accuracy, while the accuracy of the LSTM model decreased drastically.

This flow prediction method can provide the number of flights in a sector entry flow that comes from a particular upstream sector and goes to a certain downstream sector during a given future time slice. The prediction result can help ATCs better aware of the distribution of anticipated air traffic flows in the sector and develop control strategies, such as traffic re-routing and flight level allocation, in advance so that the air traffic flows can be handled in a more organized manner.

The prediction of air traffic flow in this paper only incorporates the feature of flight number in each entry flow. Various other factors can also influence airspace traffic situations, such as convective weather, airspace congestion, and operational restrictions. In the future, this traffic flow prediction method can be improved by taking more influencing factors into consideration to deliver a better prediction accuracy.

## ACKNOWLEDGMENT

This research is supported by the National Research Foundation, Singapore, and the Civil Aviation Authority of Singapore, under the Aviation Transformation Programme. Any opinions, findings and conclusions or recommendations expressed in this material are those of the author(s) and do not reflect the views of National Research Foundation, Singapore and the Civil Aviation Authority of Singapore.

## REFERENCES

- [1] F. Netjasov, "Framework for airspace planning and design based on conflict risk assessment: Part 1: Conflict risk assessment model for airspace strategic planning," *Transportation Research Part C: Emerging Technologies*, vol. 24, pp. 190–212, 2012.
- [2] J.-P. B. Clarke, S. Solak, L. Ren, and A. E. Vela, "Determining stochastic airspace capacity for air traffic flow management," *Transportation Science*, vol. 47, no. 4, pp. 542–559, 2013.
- [3] S. Gudmundsson, M. Cattaneo, and R. Redondi, "Forecasting temporal world recovery in air transport markets in the presence of large economic shocks: The case of covid-19," *Journal of Air Transport Management*, vol. 91, p. 102007, 2021.
- [4] Y. Lin, J.-w. Zhang, and H. Liu, "Deep learning based short-term air traffic flow prediction considering temporal-spatial correlation," *Aerospace Science and Technology*, vol. 93, p. 105113, 2019.
- [5] D. Chen, M. Hu, Y. Ma, and J. Yin, "A network-based dynamic air traffic flow model for short-term en route traffic prediction," *Journal of Advanced Transportation*, vol. 50, no. 8, pp. 2174–2192, 2016.
- [6] ICAO, *ICAO PANS-ATM Doc.4444, ATM/501, 15th Edition, Procedures for Air Navigation Services*. ICAO, 2010.
- [7] J. Nosedal, M. A. Piera, A. O. Solis, and C. Ferrer, "An optimization model to fit airspace demand considering a spatio-temporal analysis of airspace capacity," *Transportation Research Part C: Emerging Technologies*, vol. 61, pp. 11–28, 2015.
- [8] B. Sridhar, T. Soni, K. Sheth, and G. Chatterji, "Aggregate flow model for air-traffic management," *Journal of Guidance, Control, and Dynamics*, vol. 29, no. 4, pp. 992–997, 2006.
- [9] E. C. Fernández, J. M. Cordero, G. Vouros, N. Pelekis, T. Kravaris, H. Georgiou, G. Fuchs, N. Andrienko, G. Andrienko, E. Casado *et al.*, "Dart: a machine-learning approach to trajectory prediction and demand-capacity balancing," in *SESAR Innovation Days, Belgrade, Serbia*, 28–30 November, 2017.
- [10] I. Lymeropoulos, J. Lygeros, and A. Lecchini, "Model based aircraft trajectory prediction during takeoff," in *AIAA Guidance, Navigation, and Control Conference and Exhibit, Keystone, Colorado*, 21–24 August, 2006.
- [11] P. Wei, Y. Cao, and D. Sun, "Total unimodularity and decomposition method for large-scale air traffic cell transmission model," *Transportation research part B: Methodological*, vol. 53, pp. 1–16, 2013.
- [12] E. Gilbo and S. Smith, "A new model to improve aggregate air traffic demand predictions," in *AIAA Guidance, Navigation and Control Conference and Exhibit, Hilton Head, South Carolina*, 20–23 August, 2007, p. 6450.
- [13] D. Chen, M. Hu, H. Zhang, J. Yin, and K. Han, "A network based dynamic air traffic flow model for en route airspace system traffic flow optimization," *Transportation Research Part E: Logistics and Transportation Review*, vol. 106, pp. 1–19, 2017.
- [14] N. G. Polson and V. O. Sokolov, "Deep learning for short-term traffic flow prediction," *Transportation Research Part C: Emerging Technologies*, vol. 79, pp. 1–17, 2017.
- [15] Z. Zhang, A. Zhang, C. Sun, S. Xiang, J. Guan, and X. Huang, "Research on air traffic flow forecast based on elm non-iterative algorithm," *Mobile Networks and Applications*, vol. 26, no. 1, pp. 425–439, 2021.
- [16] G. Gui, Z. Zhou, J. Wang, F. Liu, and J. Sun, "Machine learning aided air traffic flow analysis based on aviation big data," *IEEE Transactions on Vehicular Technology*, vol. 69, no. 5, pp. 4817–4826, 2020.
- [17] R. Dalmau-Codina, B. Genestier, C. Anoraud, P. Choroba, and D. Smith, "A machine learning approach to predict the evolution of air traffic flow management delay," in *2021 ATM Seminar virtual event*, 20–24 Sep 2021.
- [18] K. W. Church, "Word2vec," *Natural Language Engineering*, vol. 23, no. 1, pp. 155–162, 2017.

- [19] D. Delahaye, A. García, J. Lavandier, S. Chaimatanan, and M. Soler, "Air traffic complexity map based on linear dynamical systems," *Aerospace*, vol. 9, no. 5, p. 230, 2022.
- [20] M. Prandini, L. Piroddi, S. Puechmorel, and S. L. Brázdilová, "Toward air traffic complexity assessment in new generation air traffic management systems," *IEEE Transactions on Intelligent Transportation Systems*, vol. 12, no. 3, pp. 809–818, 2011.
- [21] S. Samolej, G. Dec, D. Rzonca, A. Majka, and T. Rogalski, "Regular graph-based free route flight planning approach," *Aircraft Engineering and Aerospace Technology*, vol. 93, no. 9, pp. 1488–1501, 2021.
- [22] "Dsna france introduces free route airspace above 6000m," <https://centreforaviation.com/news/dsna-france-introduces-free-route-airspace-above-6000m-1106609>, accessed on February 3, 2022.
- [23] B. S. Ali and N. A. Taib, "A study on geometric and barometric altitude data in automatic dependent surveillance broadcast (ads-b) messages," *Journal of Navigation*, vol. 72, no. 5, p. 1140–1158, 2019.
- [24] C. Ma, Q. Cai, S. Alam, B. Sridhar, and V. N. Duong, "Airway network management using braess's paradox," *Transportation Research Part C: Emerging Technologies*, vol. 105, pp. 565–579, 2019.
- [25] S. C. Mohleji and G. Wang, "Modeling ads-b position and velocity errors for airborne merging and spacing in interval management application," The MITRE Corporation, Tech. Rep., 2010.
- [26] V. Amanipour and S. Ghaemmaghami, "Median filtering forensics in compressed video," *IEEE Signal Processing Letters*, vol. 26, no. 2, pp. 287–291, 2018.
- [27] D. Martínez, S. Belkoura, S. Cristobal, F. Herrema, and P. Wachter, "A boosted tree framework for runway occupancy and exit prediction," in *8th Sesar Innovation Days, Salzburg, Austria*, 3-7 Dec. 2018.
- [28] J. García-Heras Carretero, "Analysis of the geometric altimetry to support aircraft optimal trajectories within the future 4d trajectory management," Ph.D. dissertation, Aeronauticos, 2014.
- [29] K. M. Johnson, R. M. McKay, J. Etourneau, F. J. Jiménez-Espejo, A. Albot, C. R. Riesselman, N. A. Bertler, H. J. Horgan, X. Crosta, J. Bendle *et al.*, "Sensitivity of holocene east antarctic productivity to subdecadal variability set by sea ice," *Nature Geoscience*, vol. 14, no. 10, pp. 762–768, 2021.
- [30] J. Zhu, Q. Wang, C. Tao, H. Deng, L. Zhao, and H. Li, "Ast-gcn: Attribute-augmented spatiotemporal graph convolutional network for traffic forecasting," *IEEE Access*, vol. 9, pp. 35 973–35 983, 2021.
- [31] S. Guo, Y. Lin, N. Feng, C. Song, and H. Wan, "Attention based spatial-temporal graph convolutional networks for traffic flow forecasting," in *Proceedings of the AAAI Conference on Artificial Intelligence, Hawaii, USA*, vol. 33, no. 01, 27 Jan-1 Feb 2019, pp. 922–929.
- [32] J. Xie, Q. Miao, R. Liu, W. Xin, L. Tang, S. Zhong, and X. Gao, "Attention adjacency matrix based graph convolutional networks for skeleton-based action recognition," *Neurocomputing*, vol. 440, pp. 230–239, 2021.
- [33] L. Ma and Y. Zhang, "Using word2vec to process big text data," in *2015 IEEE International Conference on Big Data (Big Data), Santa Clara, CA, USA*. IEEE, 29 Oct-1 Nov, 2015, pp. 2895–2897.